https://doi.org/10.26565/2220-637X-2024-44-03 ISSN 2220-637X
УДК: 544.77+ 544.723.2

COLLOIDAL BEHAVIOR OF OXIDIZED AND LYSOZYME-COATED SINGLE-WALLED CARBON NANOTUBES. ANALYSIS VIA DYNAMIC AND ELECTROPHORETIC LIGHT SCATTERING

A. Laguta

V.N. Karazin Kharkiv National University, School of Chemistry, 4 Svobody sqr., 61022 Kharkiv, Ukraine

✉ laguta@karazin.ua https://orcid.org/0000-0002-0736-2923

The concept of surface oxidation or noncovalent coating of carbon nanotubes for successful application in aqueous fluids has a cost in terms of pollution, fate, and toxicity. Co-existing components in vitro or in vivo can influence the nanotube colloidal behavior and affect their transport. In this work, the interaction of oxidized single-walled carbon nanotubes with CsI and $Sr(NO_3)_2$ and the effect of lysozyme on the colloidal behavior of these nanotubes in aqueous systems are examined using dynamic and electrophoretic light scattering.

The concentration regimes of CsI and $Sr(NO_3)_2$ that determine the colloidal stability and instability of oxidized single-walled carbon nanotubes were identified. Oxidizing of the nanotube surface enhances colloidal stability to CsI and adsorption of Sr^{2+} cations by decorating the surface with COOH groups. Selective binding of metal cations and large specific surface area favor the removal of heavy and radioactive metals in cationic form from the bulk phase.

Biological and medical applications contribute to the fact that the interactions of carbon nanotubes with lysozyme are the object of several works. Covalent and noncovalent decoration by the enzyme creates a combination of electrical, mechanical, thermal, and optical properties of carbon nanotubes with inherent antibacterial activity of lysozyme. For example, Horn et al. reported antimicrobial fibers with four times the toughness of spider silk. However, to the best of our knowledge, little is known about colloidal stability and interaction with ions of protein-coated carbon nanotubes.

Keywords: *nanotube, lysozyme, coagulation, water pollution, hydrodynamic size, zeta potential, dynamic light scattering*

Introduction

The annual global production of carbon nanotubes for the scientific and industrial industry is estimated to be several thousand tons. The production of carbon nanotubes inevitably leads to their release into predominantly aquatic systems. The toxicity of nanotubes has been discussed in Refs. . Environmental processes can alter the nanotube state, affecting their transport, fate, and toxicity. In Ref. a hypothetical loading of nanotubes into environment systems was simulated to demonstrate the differences between exposure concentrations during the loading and recovery period.

Carbon nanotubes are characterized by a large specific surface area of 100–400 m^2/g. Nanocarbons in aqueous systems are hydrophobic colloidal dispersions. The creation of a stable colloidal system facilitates their high adsorption surface area. Fundamental concepts related to colloidal stability are modification by oxidation and surfactants-coating. Carbon nanotubes biography and degree of their surface oxidation compared in Ref. provides a rationale for controlling colloidal stability in water and consequently the environmental fate and nanotube toxicity problems. The presence of charged surface provides the basis for efficient ion exchange. Carbon nanotubes decorated with COOH groups exhibit higher adsorption efficiency for Cd^{2+}, Cu^{2+}, Pb^{2+}, and Hg^{2+} than bare ones. Selective binding of heavy metal ions, drugs, dyes, etc. leads to adsorption and hence their removal from the bulk phase. While strong binding of the pollutants is vital, an efficient nanotube coagulation methodology should also be included in the concept, otherwise, the nanoparticles remain in the water as nanovechicles. Finding an efficient protocol for sorbent separation after treatment is as important as the actual sorption process. Coagulation has the potential to remove nanocarbon derivatives with a captured species. The coagulation of carbon nanotubes by organic and inorganic electrolytes in water has been reported in Refs. .

Oxidation of carbon nanotube leads to the formation of negative surface charge in aqueous systems, which limits the sorption efficiency of anionic pollutants. In this work, the cationic enzyme lysozyme,

LSZ, was involved in surface modification. LSZ is present in all organs that are exposed to air, thus the question arises about the fate of the nanotube interface in vivo.

Noncovalent interactions between LSZ and carbon nanotubes do not disrupt the intrinsic structure of sp^2-bond and allow the production of state-of-the-art materials that combine the antibacterial propriety with mechanical, electrical, or optical properties of nanotubes. Therefore, these interactions have been the object of several works. They were investigated using scanning electron microscopy, Raman spectroscopy, circular dichroism, and fluorescence anisotropy. The tryptophan residue of lysozyme interacts favorably with sp^2-hybridized carbon nanomaterials. The surface carboxyl groups of oxidized nanotubes and amine groups of amino acid residues can form an amide bond. Adsorption of lysozyme on carboxylated, hydroxylated, and graphitized carbon nanotubes were compared in Ref. , adsorption capacity was estimated as 81800−90700 mg/g and multilayer adsorption was discussed. Antimicrobial activity of LSZ adsorbed noncovalently and attached covalently to single-walled carbon nanotubes was studied in Refs. .

The interaction of bulk ions with enzyme-coated carbon nanotubes is poorly represented in the literature. L-cysteine-coating resulted in the 89% adsorption efficiency for Cd^{2+} ions. Recently, the interactions of heavy metal salts, single-walled carbon nanotubes, and β-lactoglobulin were investigated by docking technique.

This work begins by looking at the interaction of nanotubes with Cs^+ and Sr^{2+} cations, followed by coating with lysozyme. The colloidal stability and coagulation of single-walled nanotubes coated with noncovalently bound lysozyme is studied. The sample of oxidized single-walled carbon nanotubes (D15L1–5–COOH, NanoLab, Inc., USA) with a length of 1–5 mm, a diameter of 1.5 nm, content of COOH groups of 2–7 wt.%, and a specific surface area of 220 m^2/g was used in the experiment.

Experimental

Materials

Sodium chloride, cesium iodide, strontium nitrate, sodium sulfate, calcium chloride, lysozyme from chicken egg (70000 units/mg solid, Sigma-Aldrich), and oxidized single-walled carbon nanotubes (D15L1–5–COOH, NanoLab, Inc., USA) were used as received. Energy dispersive X-ray spectroscopy, X-ray photoelectron spectroscopy, and thermogravimetric analysis were applied to characterize this sample of single-walled oxidized carbon nanotubes in Ref. .

To create the nanotube suspensions, 5 mg sample was suspended in 10 mL of distilled water with fourfold treating ultrasound for 8 min (an Ultrasonic Cleaner CD – 4800; frequency of 50/60 Hz, power of 70 W). Then the suspension was filtered through a paper filter (medium filtration rate, grade ST60, France).

The working nanotube concentration (~1 mg/L) was found spectrophotometrically (a Hitachi U–2000 spectrophotometer) according to the Bouguer–Lambert–Beer law and the extinction coefficients of 30.3 $mL \times mg^{-1} \times cm^{-1}$ and 32.3 $mL \times mg^{-1} \times cm^{-1}$ at 1033 nm and 688 nm, respectively. According to that initial dispersion contains ~160 mg/L nanotubes.

The particle hydrodynamic size, zeta-potential, and critical coagulation concentration determination procedure

The average hydrodynamic size, Z_{aver}, and polydispersity index, PdI, were generated by cumulants analysis of dynamic light scattering data obtained on a Zetasizer Nano ZS Malvern Instrument. The electrophoretic mobility was estimated by electrophoretic light scattering. Considering that electrophoretic mobility is a reflection of the effects of particle charge and diffuse double layer thickness; the electrokinetic potential in salt systems was calculated using the Henry equation (1) and the Ohshima approximation (2).

$$\zeta = u_e \times \frac{3 \times \eta}{2 \times \varepsilon_r \times \varepsilon_0} \times \frac{1}{f}, \tag{1}$$

$$f = 1 + 0.5 \times \left[1 + \frac{2.5}{\kappa \times r \times (1 + 2 \times e^{-\kappa \cdot r})} \right]^{-3}, \tag{2}$$

$$\kappa = \sqrt{\frac{2 \times F^2 \times I}{\varepsilon_0 \times \varepsilon_r \times R \times T}}, \tag{3}$$

where u_e is the electrophoretic mobility; η is the viscosity; $\varepsilon_o = 8.854 \times 10^{-12}$ F×m^{-1}; ε_r is the relative permittivity of the solvent; κ is the reciprocal Debye length; r is the radius of the colloidal particle; F is the Faraday constant; I is the ionic strength; R is the gas constant; $T = 298.15$ K.

To determine the critical coagulation concentration, CCC, the Fuchs function (4) was used.

$$W = \frac{k_r}{k_{sl}} = \frac{[(\mathrm{d}r/\mathrm{d}t)_{t\to 0}]_r}{(\mathrm{d}r/\mathrm{d}t)_{t\to 0}}, \tag{4}$$

where k_r and k_{sl} are the rate constants for rapid and slow coagulation, respectively.

The coagulation rate was determined as the slope of the time dependence of Z_{aver} for colloidal dispersions with different contents of electrolyte.

Results and discussion

The sample of oxidized single-walled carbon nanotubes (D15L1–5–COOH, NanoLab, Inc., USA) can be attributed to being the most carbonized among those studied in the literature. The ζ-potential of the colloidal particles with a diameter of an equivalent sphere of about 190 nm is –48 mV at aqueous bulk pH of 5.7. [9] According to previous study, this sample is characterized by high CCC(NaCl) value and high CCC(Na^{1+})/CCC(Ca^{2+}) ratio. Complex of Ca^{2+} with surface carboxyl commonly put forward as the reason for the excessive coagulating power.

The results obtained here for Cs^+ and Sr^{2+} extend the empirical set to highlight higher colloidal stability of oxidized nanotubes than bare ones and the enhanced coagulation power of the two charged cations. On the practical side, the results facilitate the search for effective scavengers for ^{137}Cs and ^{90}Sr as representatives of hazardous radionuclides.

It should be mentioned that the excess energy at the nanotubes surface compared to the bulk controls coagulation and adsorption. The carboxyl groups of oxidized nanotubes contribute to the formation of an electric double layer, EDL, which partially compensates for this excess energy. The high content of surface carboxyl groups also leads to surface hydration, which affects the colloidal behavior within the framework of the structural component in terms of Churaev and Derjaguin.

In terms of DLVO theory, the electric potential and EDL thickness as well as the Hamaker constants of nanotube–nanotube ($4–60 \times 10^{-20}$ J) and water–water ($3.7–5.5 \times 10^{-20}$ J) interactions mainly determine the height of the energy barrier, at the maximum of which repulsion exceeds attraction. At 40 mmol/L CsI and 1 mmol/L $Sr(NO_3)_2$, the zeta potential of nanospecies changes to –24 mV and –19 mV, respectively. In line with Powis, these EDL changes are followed by salt systems with colloidal instability regime i.e. the aggregation rate of colloidal particles is not negligible (Fig. 1). Eq. (4) implies that at indicated salt systems the double layer is thicker (by a factor of 3.7) and the ionic atmosphere is more diffuse in the case of $Sr(NO_3)_2$, thus the particle zeta potential changes further by adsorption before coagulation occurs. The electrostatic energy can then no longer stabilize the nanotube dispersion.

The concentration of CsI and $Sr(NO_3)_2$, which correspond to the beginning of the rapid coagulation regime, are given in Table 1. At these concentrations, the ζ values become –(12–10) mV (Fig. 1). The influence of the electrolyte is mainly due to the compression of EDL thickness, which makes possible the contact of particles at a distance at which the attraction forces prevail. As empirical data show, EDL compression by NaCl in Ref. and CsI occurs mainly due to a decrease in the diffusion of counterions into the bulk phase caused by an increase in the ionic strength of the system. It has been demonstrated in paper that the acid dissociation constant of surface carboxyl groups is affected by the ionic strength. Nevertheless, CCC(NaCl) > CCC(CsI), the stronger coagulation power of Cs^+ is in line with their ionic radius and hydration radius. Sr^{2+} and Ca^{2+} have similar ionic radii. However the properties of ions in the aqueous system affect characteristics such as surface tension, their adsorption, the ionization degree of acid and salt, and their interaction with carboxylic group, thus the CCCs for $CaCl_2$ and $Sr(NO_3)_2$ are different. The dications also affect both the thickness of the diffuse double layer and the surface electric potential. Here, the surface electric charge is subject to change by the adsorption of ions. For example, in the context of tools serving as complexing agents for radioactive

strontium, a montmorillonite modified by oxalate has increased (about 136% over pristine clay at pH slightly above 8) selectivity for Sr^{2+}.

Table 1. Critical rapid coagulation concentrations for 1 mg/L oxidized single-walled carbon nanotubes, SWCNT, aqueous suspension, 25 ºC, pH = 5.7

Electrolyte	**CCC**, mmol/L	
	Initial SWCNT system	SWCNT system with LSZ
NaCl	150	85 ± 5
CsI	120 ± 10	–
$CaCl_2$	1.8	45 ± 5
$Sr(NO_3)_2$	5.5 ± 0.5	–
Na_2SO_4	–	0.70 ± 0.09

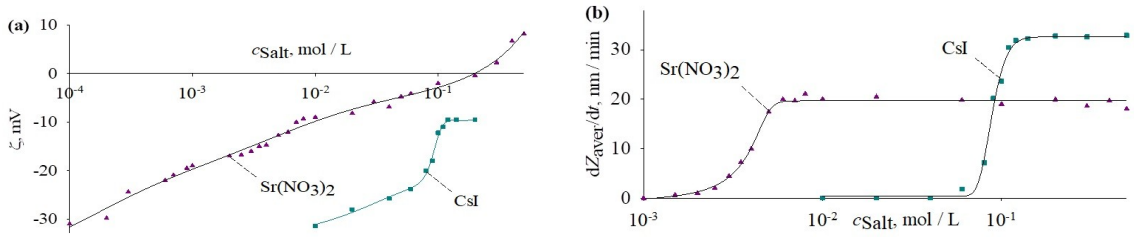

Fig. 1. Dependences of the zeta potential (a) and the rates of size increasing (b) *vs* concentrations of CsI (square) and $Sr(NO_3)_2$ (triangle) in aqueous dispersion of SWCNT.

Co-existing components in vitro or in vivo can modify the nanotube surface state, affecting their transport, fate, and toxicity. In this paper, the colloidal behavior of the nanotubes in lysozyme, LSZ, system is examined.

Lysozyme (isoelectric point of ~11) in distilled water with pH of 5.7 carries a formal positive charge (Table A1). At 2–5 mg/mL LSZ, the hydrodynamic size of nanospecies (Fig. A1**)** determined by dynamic light scattering, DLS, is smaller than that reported in Ref. according to both DLS and small angle X-ray scattering (radius of gyration of 1.49 nm). Based on Ref. , LSZ at <0.3 M NaCl is almost the same as the initial state, but at >0.3 M NaCl colloidal instability was observed and at 0.5 M NaCl aggregate size reaches about 0.7 μm. Starting with 2 ml initial suspension, 50 mg LSZ was added and the system was treated with ultrasound at a frequency of 50/60 Hz for 8 min. The created system was kept at 4 ºC. For measurements, a 160-fold dilution was. The diffusion coefficient of nanoparticles increases slightly (Fig. 2), corresponding to Z_{aver} of 225 ± 15 nm (PdI = 0.29 ± 0.01). Electrophoretic light scattering (Fig. 3) indicated a change in direction of species migration in electrophoresis, corresponding to ζ of +27±3 mV (+ is inserted for distinction). This indicates an effective modification of the nanotubes by coating the surface with the enzyme. The electrophoretic mobility is higher than reported in Ref. and in line with data from Refs. . The modified colloid was stable during several weeks of observation. The electrolyte effects on colloidal behavior was investigated.

The CCC(NaCl)/CCC($CaCl_2$) ratio is ~2 and ~83 for the system with and without LSZ (Table 1). The result corresponds to overcharging of the nanotube surface through enzyme coating and Cl^- ions cause coagulation of modified positive species. Examination of the dianion influence led to the CCC(NaCl)/CCC(Na_2SO_4) value of ~120, which exceeds the predicted effect of coagulant charge by the classical DLVO theory.

The CCC(NaCl) value for the colloid with lysozyme compared to the original system indicates a decrease in colloidal stability. According to the general idea, protein coating of the nanomaterial suggests steric hindrance. This concept prevents contact between nanoparticle surfaces at a distance at which the attraction forces prevail. However, the initial nanotube surface is oxidized, for this state, the CCC(NaCl) value is regarded as high. Considering the structure of LSZ with 129 residues the conclusion was that in the native state, 83% of the surface is hydrophobic. The carboxyl groups of nanotubes can interact with the functional group of LSZ, thus exposing the hydrophobic part to the interface. This can reduce the colloidal stability of oxidized nanotubes and the CCC(NaCl) value. This also clarifies the reduced ability to suspend nanotubes in aqueous LSZ.

The negative electrophoretic mobility for the nanotube dispersion with LSZ after 0.4 mol/L NaCl corresponds to the salt concentration at which the aforementioned enzyme aggregation was observed in the native LSZ system.

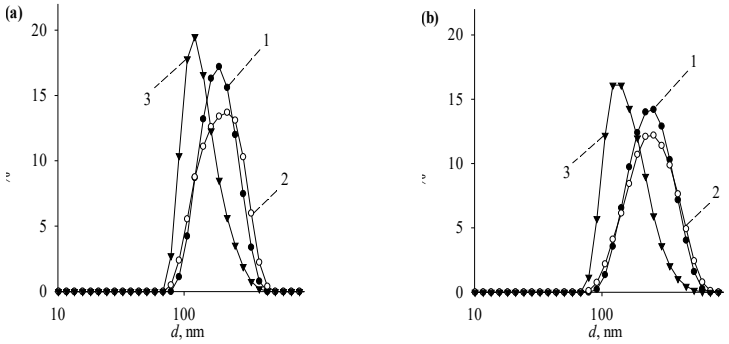

Fig. 2. Size distribution by intensity (1), volume (2), and particle number (3) of aqueous dispersions of SWCNT without (a) and with (b) lysozyme.

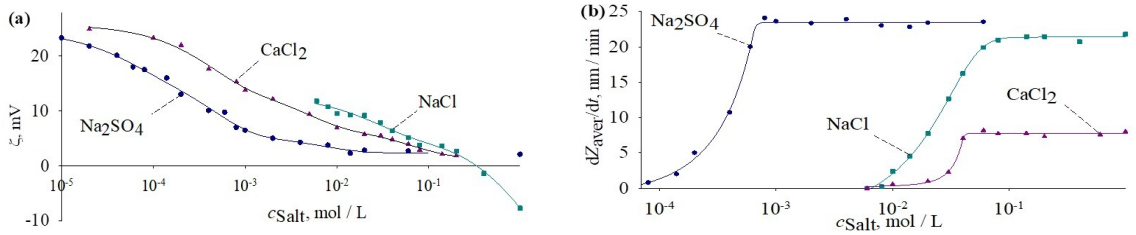

Fig. 3. Dependences of the zeta potential (a) and the rates of size increasing (b) *vs* concentrations of NaCl (square), $CaCl_2$ (triangle), and Na_2SO_4 (circle) in aqueous dispersion of SWCNT with lysozyme.

Conclusions

Hydrophobic carbon nanotubes are purposely oxidized for successful application in aqueous systems. In the colloidal state, they are subjected to further modifications by interacting with the system components. In vivo, nanotubes are exposed to a range of proteins, and it is the nanotubes complexes with polypeptide, rather than the bare nanotubes, that determine the behavior of the colloid. Various surface modifications find their application in one way or another, for example, covalent and non-covalent modification with lysozyme leads to unique structures with antimicrobial properties; compression of EDL thickness by inorganic electrolytes that reduce colloidal stability is used for sedimentation of heavy and radioactive metal ions; etc. The rational application of modified nanotubes in aqueous systems requires accounting for and controlling the morphology of the interface and the effects they generate. This work deals with the colloidal behavior of COOH-decorated nanotubes in the systems of Cs^+, Sr^{2+}, and lysozyme. Oxidized single-walled carbon nanotubes with COOH groups of content 2–7 wt.% and specific surface area of 220 m^2/g according to the information from the vendor were used.

Oxidation of the nanotube surface implies the emergence of stabilizing factors. The short-range attraction carbon nanotubes with Hamaker constant of $4–60\times10^{-20}$ J (published literature values) is balanced by long-range electrostatic repulsion (weakly screened COO^- groups) in distilled water. The colloidal stability regime was observed up to 40 mmol/L CsI and 1 mmol/L $Sr(NO_3)_2$ at which the nanospecies zeta potential becomes –24 and –19 mV, respectively, i.e. the electrostatic energy can no longer stabilize the nanotube dispersion. The rapid coagulation regime starts at 120 mmol/L CsI and 5.5 mmol/L $Sr(NO_3)_2$ and the ζ values of –(12–10) mV. The results obtained here for Cs^+ and Sr^{2+} extend the recent empirical set for Na^+, Ca^{2+}, and Ba^{2+} to highlight higher colloidal stability of oxidized nanotubes than bare ones. Along with the compression of the thickness of the diffuse double layer, the addition of the electrolytes affects the electric charge. Alteration in the magnitude of the electric charge by $Sr(NO_3)_2$ is controlled by cation adsorption. As a result, the CCC(Cs^+)/CCC(Sr^{2+}) ratio is

high. Overcharging of the nanotubes by the dications does not lead to stabilization of the colloid. From a practical point of view, these results should be taken into account in the strategy of water purification from both toxic cations and nanotubes.

Lysozyme is also noncovalently adsorbed on the nanotube surface in vitro. The surface modification was empirically observed by overcharging the surface of the dispersion particles, which was colloidally stable during several weeks of observation. As such, changing the direction of nanotube migration in a system with lysozyme, for example, is critical in electrophoresis applications; the positive formal charge of the modified surface (ζ of +27±3 mV) is useful for loading anionic forms of transition metals, drugs, etc. Steric hindrance of the coated surface generally suggests protection against short-range attraction carbon nanospecies. However, the CCCs were lower than in the lysozyme-free system. This result is expected if accepting the fact that 83% of native lysozyme is hydrophobic and interaction with carboxyl groups of nanotubes directs the hydrophobic part to the interface.

Acknowledgement

This work was financial supported by the Ministry of Education and Science of Ukraine in the frame of Project 0125U000840.

References

1. Kim M., Goerzen, D., Jena, P. V., Zeng, E., Pasquali, M., Meidl, R. A., Heller, D. A. Human and environmental safety of carbon nanotubes across their life cycle. *Nat. Rev. Mater.* **2024**, *9*(1), 63-81. https://doi.org/10.1038/s41578-024-00670-5
2. Drew R., Frangos, J., Hagen, T. Engineered nanomaterials: a review of the toxicology and health hazards. In *Safe Work Australia*, 2009.
3. Yuan X., Zhang, X., Sun, L., Wei, Y., Wei, X. Cellular toxicity and immunological effects of carbon-based nanomaterials. *Part. Fibre Toxicol.* **2019**, *16*, 1-27. https://doi.org/10.1186/s12989-019-0299-z
4. Zhang C., Wu, L., de Perrot, M., Zhao, X. Carbon nanotubes: a summary of beneficial and dangerous aspects of an increasingly popular group of nanomaterials. *Front. Oncol.* **2021**, *11*, 693814. https://doi.org/10.3389/fonc.2021.693814
5. Zhao J., Wang, Z., White, J. C., Xing, B. Graphene in the aquatic environment: adsorption, dispersion, toxicity and transformation. *Environ. Sci. Technol.* **2014**, *48*(17), 9995-10009. https://doi.org/10.1021/es5022679
6. Avant B., Bouchard, D., Chang, X., Hsieh, H.-S., Acrey, B., Han, Y., Spear, J., Zepp, R., Knightes, C. D. Environmental fate of multiwalled carbon nanotubes and graphene oxide across different aquatic ecosystems. *NanoImpact.* **2019**, *13*, 1-12. https://doi.org/10.1016/j.impact.2018.11.001
7. Birch M. E., Ruda-Eberenz, T. A., Chai, M., Andrews, R., Hatfield, R. L. Properties that influence the specific surface areas of carbon nanotubes and nanofibers. *J. Occup. Hyg.* **2013**, *57*(9), 1148-1166. https://doi.org/10.1093/annhyg/met042
8. Pashley R. M., Karaman, M. E. *Applied colloid and surface chemistry*. John Wiley & Sons: New York, 2021.
9. Laguta A., Mchedlov-Petrossyan, N., Kovalenko, S., Voloshina, T., Haidar, V., Filatov, D. Y., Trostyanko, P., Karbivski, V., Bogatyrenko, S., Xu, L. Stability of aqueous suspensions of COOH-decorated carbon nanotubes to organic solvents, esterification, and decarboxylation. *J. Phys. Chem. Lett.* **2022**, *13*(43), 10126-10131. https://doi.org/10.3390/liquids2030013
10. Anitha K., Namsani, S., Singh, J. K. Removal of heavy metal ions using a functionalized single-walled carbon nanotube: a molecular dynamics study. *J. Phys. Chem. A* **2015**, *119*(30), 8349-8358. https://doi.org/10.1021/acs.jpca.5b03352
11. Kryshtal A., Mchedlov-Petrossyan, N., Laguta, A., Kriklya, N., Kruk, A., Osawa, E. Primary detonation nanodiamond particles: Their core-shell structure and the behavior in organo-hydrosols. *Colloids Surf. A: Physicochem. Eng. Asp.* **2021**, *614*, 126079. https://doi.org/10.1016/j.colsurfa.2020.126079

12. Laguta A. N., Mchedlov-Petrossyan, N. O., Bogatyrenko, S. I., Kovalenko, S. M., Bunyatyan, N. D., Trostianko, P. V., Karbivskii, V. L., Filatov, D. Y. Interaction of aqueous suspensions of single-walled oxidized carbon nanotubes with inorganic and organic electrolytes. *J. Mol. Liq.* **2022**, *347*, 117948. https://doi.org/10.1016/j.molliq.2021.117948
13. Mchedlov-Petrossyan N. O., Kriklya, N. N., Laguta, A. N., Ōsawa, E. Stability of detonation nanodiamond colloid with respect to inorganic electrolytes and anionic surfactants and solvation of the particles surface in DMSO–H2O organo-hydrosols. *Liquids.* **2022**, *2*(3), 196-209. https://doi.org/10.3390/liquids2030013
14. Johnson L. N. The structure and function of lysozyme. *Sci. Prog.* **1966**, 367-385.
15. Horn D. W., Tracy, K., Easley, C. J., Davis, V. A. Lysozyme dispersed single-walled carbon nanotubes: interaction and activity. *J. Phys. Chem. C* **2012**, *116*(18), 10341-10348. https://doi.org/10.1021/jp300242a
16. Horn D. W., Ao, G., Maugey, M., Zakri, C., Poulin, P., Davis, V. A. Dispersion state and fiber toughness: antibacterial lysozyme-single walled carbon nanotubes. *Adv. Funct. Mater.* **2013**, *23*(48), 6082-6090. https://doi.org/10.1002/adfm.201300221
17. Borzooeian Z., Safavi, A., Hossain Sheikhi, M., Aminlari, M., Mahdi Doroodmand, M. Preparation and investigation on properties of lysozyme chemically bonded to single-walled carbon nanotubes. *J. Exp. Nanosci.* **2010**, *5*(6), 536-547. https://doi.org/10.1080/17458081003699122
18. Noor M. M., Goswami, J., Davis, V. A. Comparison of attachment and antibacterial activity of covalent and noncovalent lysozyme-functionalized single-walled carbon nanotubes. *ACS Omega* **2020**, *5*(5), 2254-2259. https://doi.org/10.1021/acsomega.9b03387
19. Piao L., Liu, Q., Li, Y. Interaction of amino acids and single-wall carbon nanotubes. *J. Phys. Chem. C* **2012**, *116*(2), 1724-1731. https://doi.org/10.1021/jp2085318
20. Du P., Zhao, J., Mashayekhi, H., Xing, B. Adsorption of bovine serum albumin and lysozyme on functionalized carbon nanotubes. *J. Phys. Chem. C* **2014**, *118*(38), 22249-22257. https://doi.org/10.1021/jp5044943
21. Taghavi M., Zazouli, M. A., Yousefi, Z., Akbari-adergani, B. Kinetic and isotherm modeling of Cd (II) adsorption by l-cysteine functionalized multi-walled carbon nanotubes as adsorbent. *Environ. Monit. Assess.* **2015**, *187*(11), 682. https://doi.org/10.1007/s10661-015-4911-x
22. Zhytniakivska O., Tarabara, U., Vus, K., Trusova, V., Gorbenko, G. Molecular docking study of protein-functionalized carbon nanomaterials for heavy metal detection and removal. *East Eur. J. Phys.* **2024**, (3), 484-490. https://doi.org/10.26565/2312-4334-2024-3-59
23. Jeong S. H., Kim, K. K., Jeong, S. J., An, K. H., Lee, S. H., Lee, Y. H. Optical absorption spectroscopy for determining carbon nanotube concentration in solution. *Synth. Met.* **2007**, *157*(13), 570-574. https://doi.org/10.1016/j.synthmet.2007.06.012
24. Hazel F. Effects of electrolytes in hydrophobic systems. I. Electric mobility and stability. *J. Phys. Chem.* **1941**, *45*(5), 731-738. https://doi.org/10.1021/j150410a002
25. Delgado Á. V., González-Caballero, F., Hunter, R., Koopal, L., Lyklema, J. Measurement and interpretation of electrokinetic phenomena. *J. Colloid Interface Sci.* **2007**, *309*(2), 194-224. https://doi.org/10.1016/j.jcis.2006.12.075
26. Fuchs N. Über die stabilität und aufladung der aerosole. *Z. Phys.* **1934**, *89*(11), 736-743. https://doi.org/10.1007/BF01341386
27. Deline A. R., Frank, B. P., Smith, C. L., Sigmon, L. R., Wallace, A. N., Gallagher, M. J., Goodwin Jr, D. G., Durkin, D. P., Fairbrother, D. H. Influence of oxygen-containing functional groups on the environmental properties, transformations, and toxicity of carbon nanotubes. *Chem. Rev.* **2020**, *120*(20), 11651-11697. https://doi.org/10.1021/acs.chemrev.0c00351
28. Myers D. *Surfaces, interfaces, and colloids.* Wiley: New York, 1999; Vol. 415.
29. Churaev N. V., Derjaguin, B. V. Inclusion of structural forces in the theory of stability of colloids and films. *J. Colloid Interface Sci.* **1985**, *103*(2), 542-553. https://doi.org/10.1016/0021-9797(85)90129-8
30. Maeno Y., Ishikawa, A., Nakayama, Y. Adhesive behavior of single carbon nanotubes. *Appl. Phys. Express.* **2010**, *3*(6), 065102. https://doi.org/10.1143/APEX.3.065102
31. Akita S., Nishijima, H., Nakayama, Y. Influence of stiffness of carbon-nanotube probes in atomic forcemicroscopy. *J. Phys. D: Appl. Phys.* **2000**, *33*(21), 2673. https://doi.org/10.1088/0022-3727/33/21/301

32. Israelachvili J. N. Intermolecular and surface forces. Academic press: **2011**.
33. Powis F. LXII.-The coagulation of colloidal arsenious sulphide by electrolytes, and its relation to the potential difference at the surface of the particles. *J. Chem. Soc., Trans.* **1916**, *109*, 734-744. https://doi.org/10.1039/CT9160900734
34. Liu X.-C., Skibsted, L. H. Strontium increasing calcium accessibility from calcium citrate. *Food Chem.* **2022**, *367*, 130674. https://doi.org/10.1016/j.foodchem.2021.130674
35. Papachristodoulou C. A., Assimakopoulos, P. A., Gangas, N. H. J. Strontium adsorption properties of an aluminum-pillared montmorillonite carrying carboxylate functional groups. *J. Colloid Interface Sci.* **2002**, *245*(1), 32-39. https://doi.org/10.1006/jcis.2001.7988
36. Ibáñez R., Almécija, M. C., Guadix, A., Guadix, E. M. Dynamics of the ceramic ultrafiltration of model proteins with different isoelectric point: comparison of β-lactoglobulin and lysozyme. *Sep. Purif. Technol.* **2007**, *57*(2), 314-320. https://doi.org/10.1016/j.seppur.2007.05.001
37. Tomita S., Yoshikawa, H., Shiraki, K. Arginine controls heat-induced cluster–cluster aggregation of lysozyme at around the isoelectric point. *Biopolymers* **2011**, *95*(10), 695-701. https://doi.org/10.1002/bip.21637
38. Nikfarjam S., Ghorbani, M., Adhikari, S., Karlsson, A., Jouravleva, E., Woehl, T., Anisimov, M. Irreversible nature of mesoscopic aggregates in lysozyme solutions. *Colloid J.* **2019**, *81*, 546-554. https://doi.org/10.1134/S1061933X19050090
39. Poznański J., Szymański, J., Basińska, T., Słomkowski, S., Zielenkiewicz, W. Aggregation of aqueous lysozyme solutions followed by dynamic light scattering and 1H NMR spectroscopy. *J. Mol. Liq.* **2005**, *121*(1), 21-26. https://doi.org/10.1016/j.molliq.2004.08.022
40. Bomboi F., Tardani, F., Gazzoli, D., Bonincontro, A., La Mesa, C. Lysozyme binds onto functionalized carbon nanotubes. *Colloids Surf. B: Biointerfaces.* **2013**, *108*, 16-22. https://doi.org/10.1016/j.colsurfb.2013.02.034
41. Siepi M., Donadio, G., Dardano, P., De Stefano, L., Monti, D. M., Notomista, E. Denatured lysozyme-coated carbon nanotubes: A versatile biohybrid material. *Sci. Rep.* **2019**, *9*(1), 16643. https://doi.org/10.1038/s41598-019-52701-9
42. Bomboi F., Bonincontro, A., La Mesa, C., Tardani, F. Interactions between single-walled carbon nanotubes and lysozyme. *J. Colloid Interface Sci.* **2011**, *355*(2), 342-347. https://doi.org/10.1016/j.jcis.2010.12.026
43. Smith S. C., Ahmed, F., Gutierrez, K. M., Rodrigues, D. F. A comparative study of lysozyme adsorption with graphene, graphene oxide, and single-walled carbon nanotubes: Potential environmental applications. *J. Chem. Eng.* **2014**, *240*, 147-154. https://doi.org/10.1016/j.cej.2013.11.030
44. Cao J., Pham, D., Tonge, L., Nicolau, D. Predicting surface properties of proteins on the Connolly molecular surface. *Smart Mater. Struct.* **2002**, *11*(5), 772. https://doi.org/10.1088/0964-1726/11/5/323
45. Blake C., Koenig, D., Mair, G., North, A., Phillips, D., Sarma, V. Structure of hen egg-white lysozyme: a three-dimensional Fourier synthesis at 2 Å resolution. *Nature.* **1965**, *206*(4986), 757-761. https://doi.org/10.1038/206757a0

Appendix. Dynamic and electrophoretic light scattering data for lysozyme aqueous solutions

Table A1. Diameter and electrophoretic mobility of species and polydispersity index of the solution at different lysozyme concentration

***c*, mg/mL**	**Mean diameter, nm**						**PdI**	**u_e, μm×cm×V^{-1}×s^{-1}**
	by Intensity			**by Volume**		**by Number**		
	I	II	III	I	II			
0.0005	–	–	–	–	–	–	1	–
0.005	390±50	–	–	390±50	–	380±40	1	0.3±0.1
0.05	50±30	–	–	50±30	–	50±30	1	0.4±0.1
2	65±10	1.3±0.2	–	1.3±0.2	–	1.2±0.2	0.9±0.1	1.3±0.1
5	189±90	35±20	1.1±0.1	1.1±0.1	–	1.0±0.1	0.58±0.01	1.4±0.1

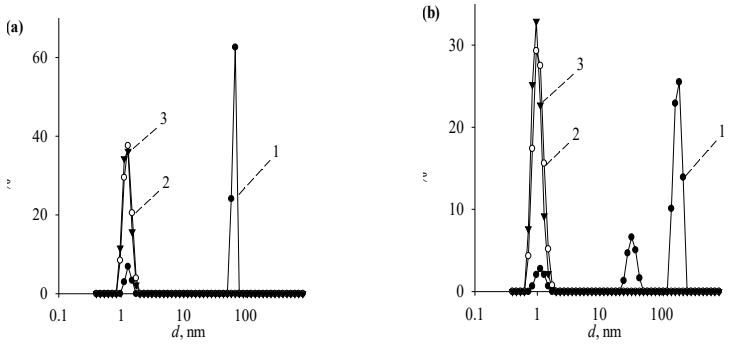

Fig. A1. Size distribution by intensity (1), volume (2), and species number (3) in 2 mg/mL (a) and 5 mg/mL (b) lysozyme aqueous solutions.

Conflict of interest: The author declares no conflict of interest.

Received 06.03.2025 *Accepted 05.05.2025*

А. Лагута. Колоїдна поведінка окислених і покритих лізоцимом одностінних вуглецевих нанотрубок. Аналіз за допомогою динамічного та електрофоретичного розсіювання світла

Харківський національний університет імені В.Н.Каразіна, хімічний факультет, майдан Свободи, 4, Харків, 61002, Україна.

Концепція поверхневого окислення або нековалентного покриття вуглецевих нанотрубок для успішного застосування у водних рідинах має свою ціну з точки зору забруднення, долі і токсичності. Співіснуючі компоненти in vitro або in vivo можуть впливати на колоїдну поведінку нанотрубок і на їхню міграцію. У цій роботі за допомогою методу динамічного та електрофоретичного розсіювання світла досліджено взаємодію окислених одностінних вуглецевих нанотрубок із CsI та $Sr(NO_3)_2$ і вплив лізоциму на колоїдну поведінку цих нанотрубок у водних системах.

Визначено концентраційні режими CsI та $Sr(NO_3)_2$, які визначають колоїдну стабільність і нестабільність окиснених одностінних вуглецевих нанотрубок. Окиснення поверхні нанотрубок підвищує колоїдну стійкість до CsI та адсорбцію Sr^{2+} за рахунок декорування поверхні COOH-групами. Селективне зв'язування катіонів металів і велика питома поверхня сприяють видаленню важких і радіоактивних металів у катіонній формі з об'ємної фази.

Біологічні та медичні застосування сприяють тому, що взаємодії вуглецевих нанотрубок із лізоцимом є об'єктом низки робіт. Ковалентне і нековалентне декорування ферментом створює комбінацію електричних, механічних, теплових та оптичних властивостей вуглецевих нанотрубок із притаманною лізоциму антибактеріальною активністю. Наприклад, Хорн та ін. повідомили про антимікробні волокна, що в чотири рази перевищують міцність павутинного шовку. Однак, наскільки нам відомо, про колоїдну стабільність і взаємодію з іонами вуглецевих нанотрубок, покритих білком, відомо небагато.

Ключові слова: *нанотрубка, лізоцим, коагуляція, забруднення води, гідродинамічний розмір, дзета-потенціал, динамічне розсіювання світла.*

Конфлікт інтересів: автор повідомляє про відсутність конфлікту інтересів.

Надіслано до редакції 06.03.2025 *Прийнято до друку 05.05.2025*